Calculation of Auger spectra for liquid metals

G Hörmandinger†§, J Hafner‡, W Jank‡ and P Weinberger†

†Institut für Technische Elektrochemie, Technische Universität Wien, A-1060 Wien, Austria
‡Institut für Theoretische Physik, Technische Universität Wien, A-1040 Wien, Austria

Abstract. A method for calculating core–core–valence and core–valence–valence Auger spectra using the results of electronic structure calculations is applied to liquid tin. Our calculations allow for an interpretation of the Auger spectra in terms of the partial densities of states.

1. Introduction

Recently considerable progress has been achieved in the investigation of the electronic structure of molten metals [1–9]. It is now evident that neither the simplifying picture of a free-electron-like density of states, nor the equally oversimplified view of a close similarity of the electronic properties of the crystalline and liquid phases are correct. Of particular interest are the electronic properties of the heavy polyvalent metals that show a pronounced change of the local environment of an atom on melting. In liquid Ge, for example, a deep pseudogap about 4 eV below the Fermi level separates the valence band into a low-lying s band and a p band in the vicinity of the Fermi edge [1, 5]. This is in striking contrast to the band structure of the crystalline phases: the semiconducting (diamond-type) phase is characterized by a strong sp^3 hybridization; in the metallic high-pressure phases (β-tin type, simple hexagonal) the broadening of the bands leads to a decrease of sp^3 hybridization and finally to a free-electron-like DOS. Similar effects are observed in Sn, Ga, Sb, and Bi. Despite their complexity, the trends in the electronic structure of the liquid elements and their relation to the trends in the liquid structure are now well understood. This understanding has been achieved by combined progress in theory and experimentation: it is now possible to produce high-resolution photoelectron spectra [1–3] and to compare them with self-consistent electronic structure calculations based on realistic structural models [4–9]. Of particular value is the possibility of calculating the partial photoionization cross-sections for the liquid as a function of the energy of the exciting photon and of the binding energy of the emitted electron [7, 8, 10, 11]. The calculation of the cross-section is based on the assumption that the wavevector is not a conserved quantity. In the crystal this approximation is justified only for the high excitation energies of x-ray photoelectron spectroscopy, but in the liquid phase it applies independently of the excitation energy. It is primarily the quantitative comparison of the measured

§ Present address: Imperial College of Science and Technology, London, UK.

and calculated photoemission intensities for different photon energies that allows for the assessment of the validity of current theoretical predictions for the electronic structure of liquid metals.

Additional information on the structure of the valence band comes from Auger electron spectroscopy (AES) involving valence electrons (core–core–valence (CCV) and core–valence–valence (CVV) transitions). In a CCV transition an initial core hole is filled by a core (valence) electron and the energy is transferred to another valence (core) electron, which is emitted. The Auger intensity for a CCV transition is an image of the partial DOS of the valence band, modified by the energy-dependent Auger transition probability. In a CVV transition two valence electrons are involved, so the Auger intensity is essentially a self-convolution of the valence-band DOS. This means that CVV Auger spectra yield only indirect information on the electronic structure.

In the present paper we present the first calculation of Auger spectra for a liquid metal, based on the techniques developed for the calculation of the Auger intensities in crystalline systems [12, 13].

2. Theory of the Auger transition probabilities

The Auger transition probability may be written as [14]

$$P = (2\pi/\hbar)|D - E|^2 \, \delta(\epsilon_3 - \epsilon_1 + \epsilon_4 + \epsilon_2). \tag{1}$$

The matrix elements D and E for the direct and exchange processes are given by

$$D = \iint \psi_1^*(r_1)\psi_2^*(r_2) \frac{e^2}{|r_1 - r_2|} \psi_3(r_1)\psi_4(r_2) \, d^3r_1 \, d^3r_2 \tag{2}$$

$$E = \iint \psi_1^*(r_1)\psi_2^*(r_2) \frac{e^2}{|r_1 - r_2|} \psi_4(r_1)\psi_3(r_2) \, d^3r_1 \, d^3r_2 \tag{3}$$

The index 1 stands for the state of the initial core hole, 2 for the state of the emitted electron. In a CCV transition the index 3 labels a core state and 4 a valence-band state; in a CVV transition both 3 and 4 stand for valence states. The calculation of the total transition probability involves summation over the magnetic quantum numbers of the core states and over all valence states. All core states are described by free-atom wave functions; the continuum state ψ_2 is described by a time-reversed LEED (lower-energy electron diffraction) state within the single-scatterer–final- state approximation [10]. After taking the square of the matrix elements, each wave function appears twice, with different r-space arguments. Thus, and by using a formal splitting of the delta function according to

$$\delta(\epsilon_3 - \epsilon_1 + \epsilon_4 - \epsilon_2) = \int d\epsilon \, \delta(\epsilon_3 - \epsilon_1 + \epsilon - \epsilon_2)\delta(\epsilon - \epsilon_4) \tag{4}$$

a spectral representation of the imaginary part of the Green's function can be introduced. The remaining steps follow the theory outlined in [12] and [13]: (i) the

Greens function is replaced by the scattering path operator [15]; and (ii) the imaginary part of the scattering path operator is expressed in terms of the angular-momentum-decomposed density of states $n_\ell(\epsilon)$.

As a result, the transition probability for CCV processes can be written as a weighted average of the ℓ-dependent DOS [12],

$$P(\epsilon) = \sum_\ell \sigma_\ell(\epsilon) n_\ell(\epsilon) \tag{5}$$

and that for CVV processes in terms of a self-convolution integral of the DOS [13]

$$P(\epsilon_2) = \sum_{\ell, \ell'} \int d\epsilon \; \sigma_{\ell\ell'}(\epsilon_1 \epsilon_2) n_\ell(\epsilon) n_{\ell'}(\epsilon_1 + \epsilon_2 - \epsilon). \tag{6}$$

The matrix elements contain integrals over the radial wave functions and Clebsch–Gordan coefficients from the angular integrations; for any details refer to earlier work.

The theory outlined here involves several approximations: (i) the neglect of the interaction of the two final-state holes; (ii) the assumption that the outgoing electron undergoes no further scattering (single-scatterer–final-state approximation); and (iii) the neglect of surface effects. We are going to apply the theory to liquid Sn. In such a heavy metal the hole–hole interaction should be relatively well screened. The single-scatterer–final-state approximation has been found to give good results for the photoemission spectra of liquid metals [6–8], and we expect surface effects to be less pronounced in liquid than in crystalline materials.

3. Application to liquid tin

The selfconsistent linear-muffin-tin-orbital (LMTO) potentials and partial densities of states used in the present calculations were taken from [5]. These calculations were performed for 'supercells' containing an instantaneous configuration of 64 tin atoms generated by a molecular dynamics simulation. The calculations were performed for the full star of four special k-points of the full Brillouin zone corresponding to the cubic supercell; a configuration average over a small number of independent configurations was taken. Figure 1 shows the total and partial densities of state and the calculated XPS spectrum, compared with experiment. Note that the partial DOS suggest a nearly complete separation of the valence band into s and p bands.

3.1. CCV spectra

Figure 2 shows the matrix elements for several CCV transitions corresponding to equation (5). We find that for transitions involving the 3d core states, the largest contribution to the Auger intensity comes from the d component of the valence-band DOS. Therefore, in view of the small d-electron contribution to the valence band, the similarity of the Auger spectrum (figure 3) to the total DOS is rather coincidental. For transitions involving the 3p core state, the s and p contribution to the matrix element is dominant, but depends rather strongly on the energy. This energy dependence causes a certain distortion of the low-energy part of the M_3N_1V spectrum compared with the total DOS, but otherwise matrix element effects are rather small.
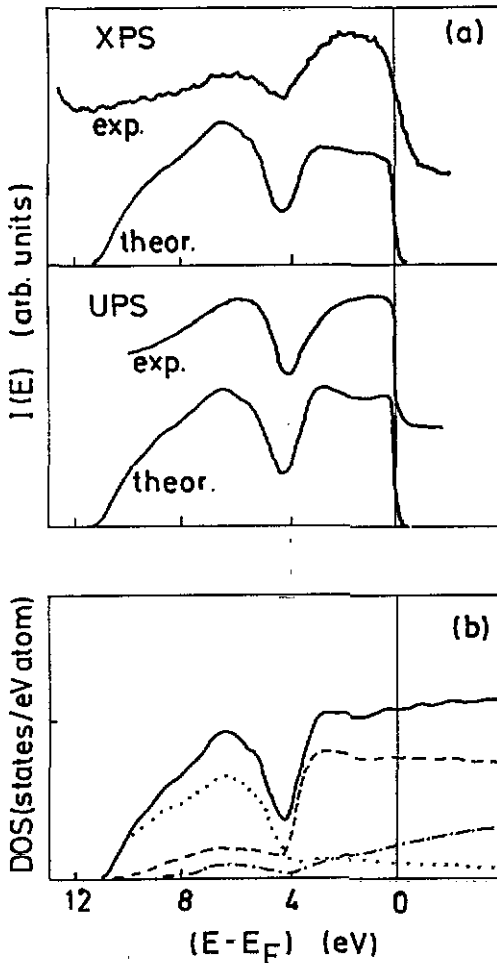
Figure 1. (a) Calculated and measured XPS and UPS ($h\nu = 40.8$ eV) spectra. (b) Total and angular-momentum-decomposed densities of states in liquid tin. Full line: total DOS; dotted: s-electron contribution; dashed: p-electron contribution; dot-dashed: d-electron contribution.

3.2. CVV spectrum

Figure 4 shows the calculated intensities for MVV and NVV Auger spectra. As expected, the width of the spectra corresponds to about two times the band width. The individual spectra are strongly influenced by matrix element effects. In the 4sVV and 4pVV spectra, the dominant $\sigma_{ll'}(\epsilon)$ matrix elements are s|s and s|p; in the 3dVV spectra they are the s|d, p|d and d|d contributions. The spectra show one single peak with small side structures. The dominant matrix elements are s|d and p|d. The strong structure in the spectrum reflects the structure in the DOS.

For a comparison with experiment, spin–orbit coupling should be taken into account. Figure 5 shows a superposition of the two 4dVV spectra (with relative weights of 2:3), shifted by a spin–orbit splitting of 1.12 eV. The 4dVV spectrum has been measured by Indlekofer [3], but unfortunately the published data cover only a range of a few eV from the onset of the transition. In this limited region the comparison
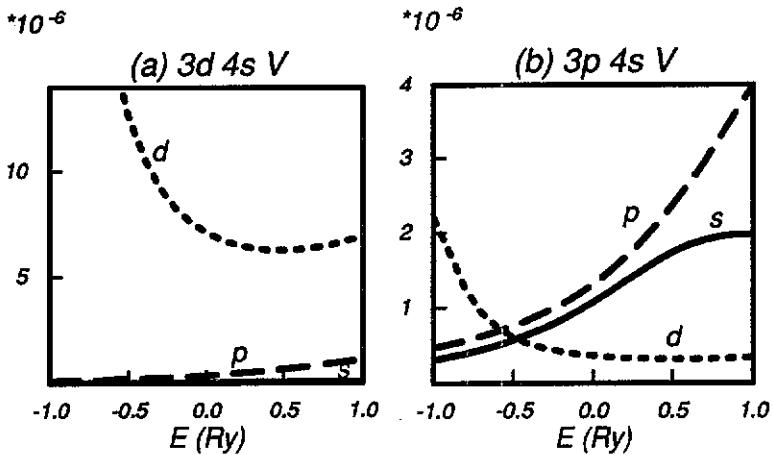
Figure 2. Matrix elements $\sigma_\ell(\epsilon)$ for CCV Auger transitions for $\ell = 0, 1, 2$. (*a*) 3d–4s–V transition; (*b*) 3p–4s–V transition. The energy scale corresponds to the LMTO potentials.
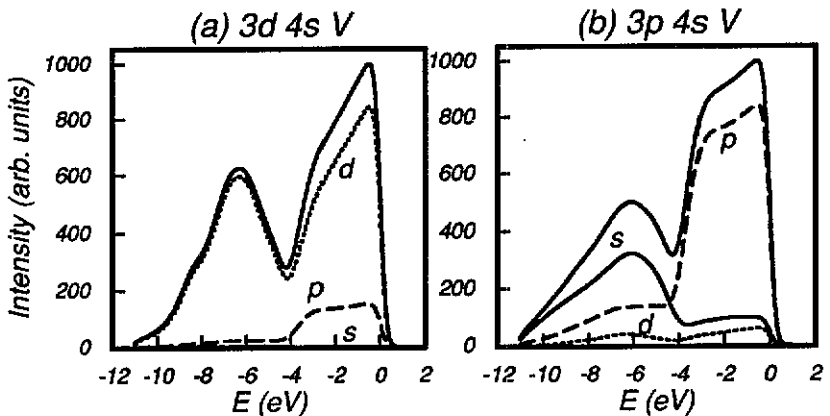

Figure 3. CCV Auger spectra for liquid tin: (*a*) 3d–4s–V; (*b*) 3p–4s–V spectrum. The zero of the energy scale is the Fermi energy.

of theory and experiment is encouraging. The remaining NVV transitions have very low intensity; the 3dVV Auger line overlaps with the 3p core-level photoemission spectrum. Within the limited energy range covered by the experiment, there are only very small differences between the Auger spectra of the solid and liquid phases. This is not unexpected, because the partial DOS of Sn are rather similar in the liquid and the crystalline β-tin phases [4]. In both cases, we find a low-lying band of s character, separated by a pseudogap at ~ 4 eV binding energy from a p band at the Fermi level (see also figure 1). The self-convolution of this split DOS leads precisely to the four-peak structure of the NVV spectrum, in the crystalline as well as in the liquid state. The discussion of the electronic spectra confirms the conclusion drawn from the simulation of the liquid structure that the short-range atomic arrangement is similar in the liquid and crystalline phases.
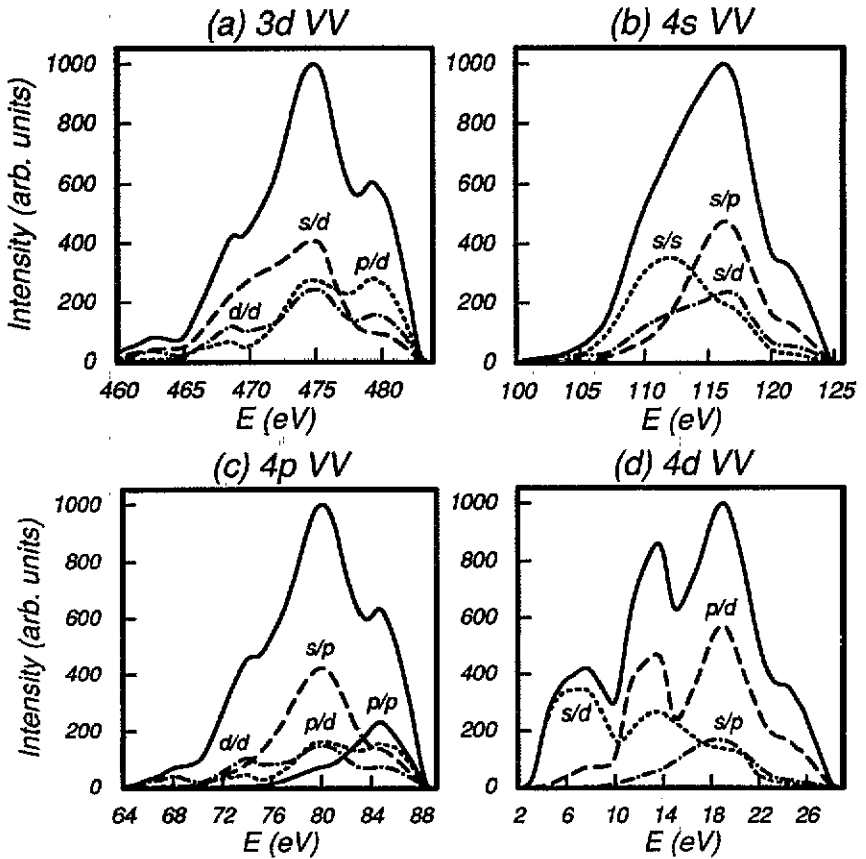
Figure 4. CVV Auger spectra for liquid tin: (*a*) 3d–V–V; (*b*) 4s–V–V; (*c*) 4p–V–V; (*d*) 4d–V–V. A spectrometer resolution of 0.6 eV has been assumed.

4. Conclusions

Up to now, Auger electron spectroscopy has been used mainly as a technique for chemical analysis, using the energetical positions of peaks to identify elements and using the relative peak intensities to determine the chemical composition. However, Auger spectra for solids and liquids carry much more information—in particular information on the structure of the valence band. To date, this information has hardly been exploited at all.

The possibility of calculating theoretical spectra in the form of weighted averages over ℓ-dependent local densities of states for CCV spectra and of weighted averages over self-convolution integrals of the DOS for CVV spectra makes it possible to exploit the valence-band information contained in the Auger spectra. Previous publications [12, 13] have demonstrated the potential of this method for crystalline solids. The present paper presents the first theoretical Auger spectra for a liquid metal. Admittedly, the database for comparison with experiment is still quite small. The reason for the lack of experimental data is (besides the intrinsic difficulty of any spectroscopy experiment on a liquid sample) the lack of reliable theoretical prediction. For example, the experimental spectrum shown in figure 5 was truncated at about 17 eV, because
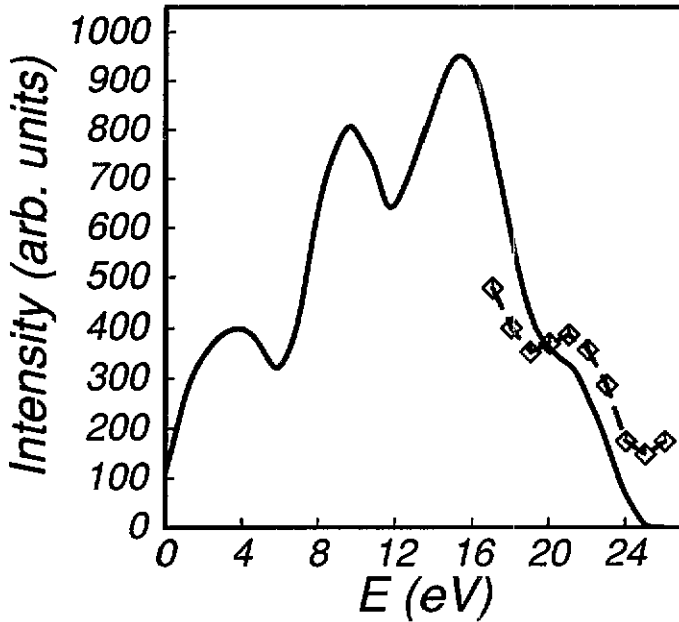
Figure 5. The calculated $N_{4,5}$VV Auger spectrum for liquid tin, compared with results from the experiment described in [3].

the intensity recorded at lower energy was considered as a background rather than an integral part of the NVV Auger spectrum. We hope that our paper will stimulate new experiments.

Acknowledgments

References

[1] Oelhafen P, Indlekofer G and Güntherodt H J 1988 Z. *Phys. Chem.* **157** 483
[2] Indlekofer G and Oelhafen P 1990 *J. Non-Cryst. Solids* **117+118** 340
[3] Indlekofer G 1988 *PhD Thesis* Universität Basel
[4] Jank W and Hafner J 1990 *Phys. Rev.* B **41** 1497; 1990 *Phys. Rev.* B **42** 6926
[5] Hafner J and Jank W 1990 *Phys. Rev.* B **42** 11530; 1992 *Phys. Rev.* B **45** 2739
[6] Jank W and Hafner J 1990 *J. Phys.: Condens. Matter* **2** 5065
[7] Jank W and Hafner J 1991 *J. Phys.: Condens. Matter* **3** 6947
[8] Hafner J and Jank W 1991 *J. Phys.: Condens. Matter* **3** SA239
[9] Jank W, Hausleitner C and Hafner J 1991 *J. Phys.: Condens. Matter* **3** 4477
[10] Redinger J, Marksteiner P and Weinberger P 1986 Z. *Phys.* B **63** 321
[11] Jarlborg T and Nilsson P O 1979 *J. Phys. C: Solid State Phys.* **12** 265
[12] Hörmandinger G, Weinberger P, Marksteiner P and Redinger J 1988 *Phys. Rev.* B **38** 1040
[13] Hörmandinger G, Weinberger P and Redinger J 1989 *Phys. Rev.* B **40** 7989
[14] Chattarji D 1976 *The Theory of Auger Transitions* (London: Academic)
[15] Faulkner J S and Stocks G M 1980 *Phys. Rev.* B **21** 3222
[16] Oelhafen P 1991 Private communication